p-ISSN 2089 – 0133 e-ISSN 2477-6416
URL : https://jurnal.uns.ac.id/ijap/article/view/67837

DOI : https://doi.org/10.13057/ijap.v13i1.67873

FT-IR SPECTRAL MODEL OF POLYESTER-COTTON FABRICS WITH CORONA PLASMA TREATMENT USING ARTIFICIAL NEURAL NETWORKS (ANNS)

Irwan Irwan[1], Juliany Ningsih Mohamad[2] and Valentinus Galih Vidia Putra*[1]
[1]Basic and Applied Science Research Group in Theoretical and Plasma Physics, Department of Textile Engineering, Politeknik STTT Bandung, Bandung, Indonesia.
[2] Applied Physics Research Group, Universitas Nusa Cendana, Kupang, Indonesia.
*Corresponding author: valentinus@kemenperin.go.id

ABSTRACT

Corona plasma technology has been studied as a surface modification for the adhesive bonding of polymers. Although corona plasma (C.P.) is becoming more popular in nanotechnology, the influence of corona plasma treatment parameters on the FT-IR spectra is a problem that has yet to be addressed. The purpose of this study was to use an artificial neural network to study the influence of corona plasma (C.P.) treatment parameters on textile polymer and evaluate the ability of this model to predict FT-IR spectral information from FT-IR measurements. In this study, polymers were modified under various corona plasma treatment conditions. We investigated FT-IR spectra information of polymers from FT-IR measurements by varying corona plasma treatment variables. We used three input parameters in this study: wavenumber, voltage, and exposure time—two output parameters: fabric roughness with SEM according to the degree of smoothness and percent transmission with FT-IR. The novel aspect of this study is that we used ANN to model the plasma treatment on polyester-cotton fabrics and the FT-IR spectra accurately enough for the first time. According to this study, the model that used four nodes (neurons) in the hidden layer, three input parameters (x_1,x_2,x_3), and 20 iterations is appropriate for determining fabric surface roughness (S.R.) and percent transmission (T%). Based on this research, the values of R^2 for determining fabric surface roughness (S.R.) and percent transmission (T%) were 99.79 percent and 67.18 percent, respectively. The results showed that the developed ANNs could accurately predict the experimental data in detail. This study is significant because it uses artificial intelligence to calculate and simulate the FT-IR spectra and fabric surface roughness of plasma treatment on textile fabrics. This study's scientific application is that it will help experts, researchers, and engineers understand the implications of plasma on the chemical structure of textile materials.

Keywords: Plasma; ANN; FT-IR; Fabric; Textile

INTRODUCTION

Polyester blends, such as polyester-cotton fabrics, are highly useful in textile industries. Compared to cotton, these fabrics have higher tensile strength, elasticity, lightness, fewer wrinkles, and are faster to dry[1]. In the textile industry, chemical processes are the most common way to improve the surface characteristics of fabrics. However, in recent years, various alternative environmentally friendly processes have been sought to reduce the use of chemicals[2]. Advanced plasma processing has been promoted as a green technology capable of changing the chemical structure and morphology of polymeric materials such as textiles [2-4]. Fourier transform infrared spectroscopy (FT-IR) measurements of polymer chemical bonding play an essential and unavoidable role in applying surface modification and work of adhesion with plasma technology in several nanotechnology studies[5]. It is difficult and time-consuming to determine the relationship between plasma process input parameters and polymer chemical bonding information from FT-IR. A modeling approach is required to estimate chemical bonding information from FT-IR for plasma-treated and non-plasma-treated materials to explain the relationship between input parameters and chemical bonding information [4, 5, 6, 7]. Several researchers [8, 9, 10] reported the effect of plasma treatment on polymeric material using surface analysis with FT-IR. The results of FT-IR spectra of plasma-treated and non-plasma-treated polymers were described as reproducible fingerprint-like patterns and varied by polymer type. Using the FT-IR technique, many studies have classified or identified plasma's effect on various polymers [8, 9, 10]. However, there have been no previous reports using FT-IR spectroscopy to identify the systemic effect of plasma on textile polymers using artificial intelligence modeling. Murru et al. [11] used a machine learning algorithm and FT-IR spectroscopy modeling to identify the chemical variables associated with grape ripeness and variety classification. The study's findings indicated that ANN could effectively identify system behavior in the presence of nonlinear data using FT-IR spectroscopy.

In epidemiological studies, Nie et al. [12] stated that FT-IR Spectroscopy and artificial neural networks could be used to identify Fusarium Organisms. According to the study's findings, FT-IR spectroscopy combined with artificial neural networks (ANNs) was well suited for defining system behavior in the presence of nonlinear data. For modeling physical phenomena in nanotechnology, several methods were developed, including adaptive neuro-fuzzy inference systems (ANFIS), response surface methodology (RSM), and artificial neural networks (ANNs)[11, 12, 13, 14]. In the last few years, response surface methodology (RSM) was used to model system behavior in the presence of nonlinear data, but this technique sometimes fails to simulate system behavior when confronted with complex and nonlinear data [13, 14]. Although the response surface method works reasonably well, its accuracy drops as the independent variable increases. Therefore, nonlinear models based on machine learning models, such as artificial neural networks (ANNs), help address complex cases, nonlinear problems, and quality control [15, 16, 17, 18, 19, 20]. The purpose of this study is to use an artificial neural network to study the influence of corona plasma (C.P.) treatment parameters on textile polymer and evaluate the ability of this model to predict the FT-IR spectral information from FT-IR measurements. The novelty of this study is that we used ANN to model the plasma treatment on textile fabrics and the FT-IR spectral measurements accurately enough for the first time. The developed ANNs could predict the experimental data in detail accurately. This study is significant because it uses artificial intelligence to calculate and simulate the FT-IR spectral measurements and fabric surface roughness of plasma treatment on textile fabrics. This research will aid practitioners, researchers, and engineers in understanding the impact of plasma on the chemical structure of textile materials.

METHODS

Materials

Tetoron Cotton 85%, or T.C. 85% Fabric, is a polyester/cotton blend composed of 85% polyester and 15% cotton. The materials used in this experiment were hydrophobic polyester-cotton (T.C. 85%) woven materials with a warp construction of 65 strands/inch and a weft count of 50 strands/inch. The warp-weft yarn count was 20 tex or 20 g/km in a 1/1 plain weave. The polyester-cotton material (T.C. 85%) with a density of 239 g/m^2 was purchased from the traditional Indonesian market.

Instrumentations

Corona plasma generator was made utilizing multi-point and flat electrodes. The machine in this study was carried out in the instrumentation physics laboratory, Politeknik STTT Bandung, The Ministry of Industry of the Republic of Indonesia. Twenty-five tipped bolts were used as multi-point electrodes, and the electrodes were connected to the power source. Scanning electron microscopy (SEM) and a Fourier transform infrared (FT-IR) spectrometer were used to examine untreated and plasma-treated fabrics' surface morphology and chemical bonding information at the Textile Research Center, The Ministry of Industry of the Republic of Indonesia. Figure 1 depicts the corona plasma machine used in this research.

The fabric samples were placed on a flat electrode in the plasma chamber, and the processing time and voltage were set. The plasma wave was formed using a high D.C. voltage of 3 kV, a room temperature of 27-28°C, an electrode distance of 4.5 cm, atmospheric conditions, and an ambient air medium. In addition, the fabric surfaces were modified using a corona discharge plasma treatment for two minutes (sample A) and three minutes (sample B) at the same voltage of 3 kV. After treatment with corona plasma, samples were placed at room temperature and atmospheric pressure and examined by scanning electron microscopy (SEM) and a Fourier transform infrared (FT-IR) spectrometer. In this study, we used three input parameters: wavenumber, applied voltage, and exposure time, and two output parameters: fabric roughness level with SEM and percent transmission with FT-IR. Fabric roughness was classified according to the degree of smoothness by using the evenness intensity of grayscale, symbolized as 0 for control fabric with average intensity at 87.8855, symbolized as 0.5 for sample A with average intensity at 90.5119, and symbolized as 1 for sample B with average intensity at 101.2784.

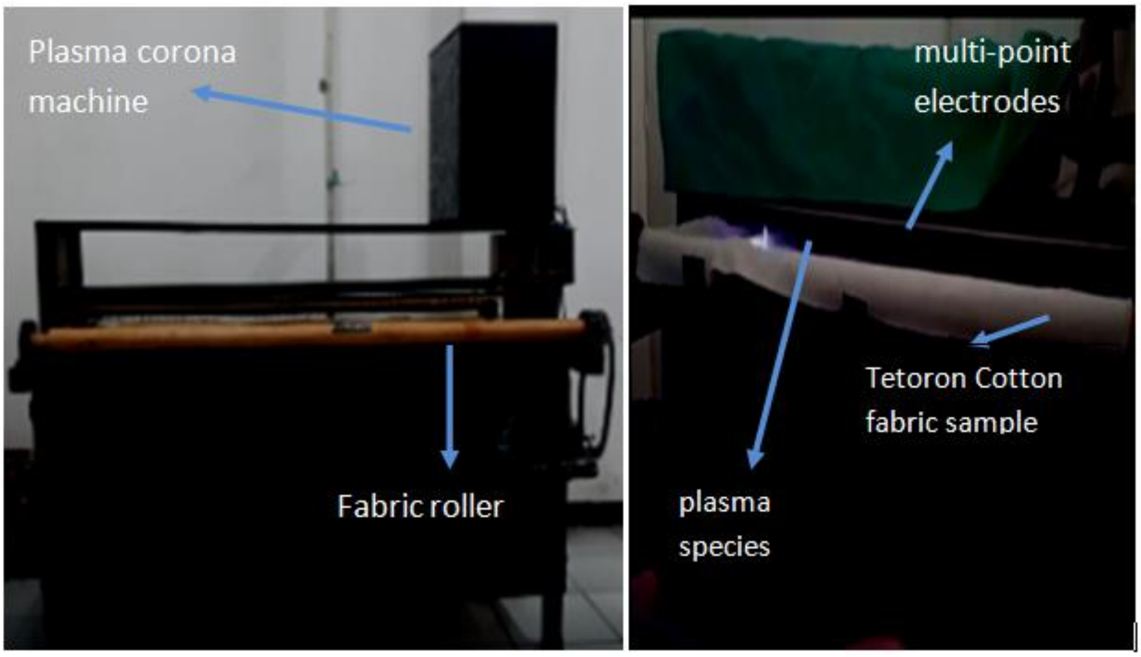

Figure 1. The prototype of the plasma machine (Physics Laboratory, Politeknik STTT Bandung).

Modeling with artificial neural networks

We used the neural network architecture developed by several physicists and chemists [15, 16, 17, 18, 19, 20]. As inputs to the model, this study used chemical bonding information from FT-IR measurements and plasma processes, such as wavenumber, voltage, and exposure time. As output parameters, fabric surface roughness (S.R.) and percent transmission (T%) were measured by SEM and FT-IR, respectively. Two parameters were considered for optimizing the models: the number of hidden neurons and training iterations. In this study, we used several nodes in which each node in the neural network, also called a neuron or perceptron, is a computational unit with one or more weighted input connections, a transfer function that combines the inputs in some way, and an output connection. The model was trained using FT-IR chemical bonding measurements and scanning electron microscopy (SEM), as seen in Figure 3 and Figure 4, respectively.

Modeling with a hidden layer with four neurons

This model considered the artificial neural networks consisting of a hidden layer with four nodes, three normalized inputs, and two normalized output neurons. The activation function of the hidden neuron adopted the sigmoid function, and the output neuron adopted a linear function, as shown in Figure 2. For better optimization, we used a constant learning rate (α=0.9) in the architecture and 20 iterations in this model.

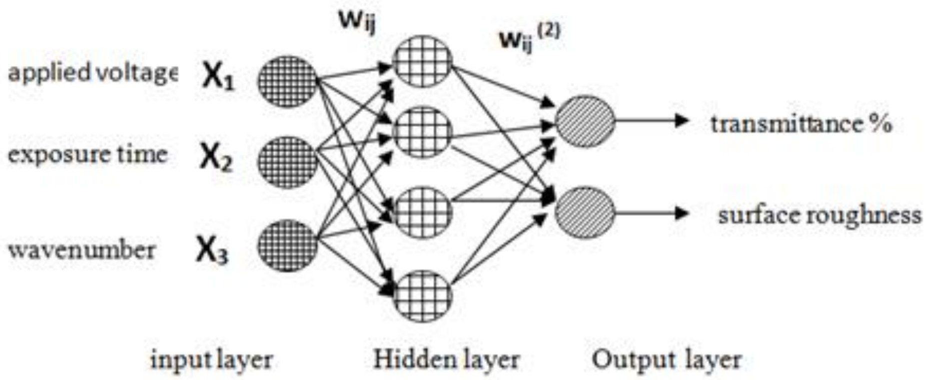

Figure 2. The model of artificial neural network architecture.

The circles and arrows in Figure 4 represent neurons and signal flows. The terms x_1, x_2, and x_3 were inputs; The terms w_{ij} and $w_{ij}{}^2$ are the weight matrices of the first and second layers, respectively. The following formula can calculate the weighted sum from Eqs. (1) and (2).

$$v_i = \sum \sum w_{ij} x_j + b_i \tag{1}$$

$$\begin{pmatrix} v_1 \\ v_2 \\ v_3 \\ v_4 \end{pmatrix}_{4\times1} = \begin{pmatrix} w_{11} & w_{12} & w_{13} \\ w_{21} & w_{22} & w_{23} \\ w_{31} & w_{32} & w_{33} \\ w_{41} & w_{42} & w_{43} \end{pmatrix}_{4\times3} \begin{pmatrix} x_1 \\ x_2 \\ x_3 \end{pmatrix}_{3\times1} + \begin{pmatrix} b_1 \\ b_2 \\ b_3 \\ b_4 \end{pmatrix}_{4\times1} \tag{2}$$

The node enters the weighted sum into the activation function (the sigmoid function, φ) and generates its output as in Eq. (3):

$$\begin{pmatrix} o_1 \\ o_2 \\ o_3 \\ o_4 \end{pmatrix}_{4\times1} = \begin{pmatrix} \varphi(v_1) \\ \varphi(v_2) \\ \varphi(v_3) \\ \varphi(v_4) \end{pmatrix}_{4\times1} \tag{3}$$

Eq. (3) is the input of the second layer. We obtain the weighted sum in the second layer, as shown in Eqs. (4) and (5).

$$\mu_i = \sum\sum w_{ij}{}^{(2)} o_j + b_i{}^{(2)} = \sum\sum w_{ij}{}^{(2)} \varphi(v_j) + b_i{}^{(2)} \tag{4}$$

$$\begin{pmatrix} \mu_1 \\ \mu_2 \end{pmatrix}_{2\times1} = \begin{pmatrix} w_{11}{}^{(2)} & w_{12}{}^{(2)} & w_{13}{}^{(2)} & w_{14}{}^{(2)} \\ w_{21}{}^{(2)} & w_{22}{}^{(2)} & w_{23}{}^{(2)} & w_{24}{}^{(2)} \end{pmatrix}_{2\times4} \begin{pmatrix} \varphi(v_1) \\ \varphi(v_2) \\ \varphi(v_3) \\ \varphi(v_4) \end{pmatrix}_{4\times1} + \begin{pmatrix} b_1{}^{(2)} \\ b_2{}^{(2)} \end{pmatrix}_{2\times1} \tag{5}$$

The neuron enters the weight matrix into the linear function and generates its output. The output activation function determines neuron behavior and can be written as in equation (6):

$$y = \begin{pmatrix} \psi(\mu_1) \\ \psi(\mu_2) \end{pmatrix}_{2x1} = \psi\left(\begin{pmatrix} w_{11}{}^{(2)} & w_{12}{}^{(2)} & w_{13}{}^{(2)} & w_{14}{}^{(2)} \\ w_{21}{}^{(2)} & w_{22}{}^{(2)} & w_{23}{}^{(2)} & w_{24}{}^{(2)} \end{pmatrix}_{2\times4} \begin{pmatrix} \varphi(v_1) \\ \varphi(v_2) \\ \varphi(v_3) \\ \varphi(v_4) \end{pmatrix}_{4\times1} + \begin{pmatrix} b_1{}^{(2)} \\ b_2{}^{(2)} \end{pmatrix}_{2\times1} \right) \tag{6}$$

The aim of training the network in this method was to adjust the weights. The weights were adjusted by minimizing the sum of the squares. The neural network was trained by providing input and output designs to it. We used the back-propagation learning algorithm and neural network models to make the model. This algorithm updates the weight values when the performance function rapidly decreases.

Modeling with a hidden layer with eight neurons

This model considered the artificial neural networks consisting of a hidden layer with eight nodes, three normalized inputs, and two normalized output neurons. The activation function of the hidden neuron adopted the sigmoid function, and the output neuron adopted a linear function. For better optimization, we used a constant learning rate (α=0.9) in the architecture and 20 iterations in this model. The following formula can calculate the weighted sum from Eqs. (7) and (8).

$$v_i = \sum\sum w_{ij} x_j + b_i \tag{7}$$

$$\begin{pmatrix} v_1 \\ v_2 \\ v_3 \\ v_4 \\ v_5 \\ v_6 \\ v_7 \\ v_8 \end{pmatrix}_{8\times1} = \begin{pmatrix} w_{11} & w_{12} & w_{13} \\ w_{21} & w_{22} & w_{23} \\ w_{31} & w_{32} & w_{33} \\ w_{41} & w_{42} & w_{43} \\ w_{51} & w_{52} & w_{53} \\ w_{61} & w_{62} & w_{63} \\ w_{71} & w_{72} & w_{73} \\ w_{81} & w_{82} & w_{83} \end{pmatrix}_{8\times3} \begin{pmatrix} x_1 \\ x_2 \\ x_3 \end{pmatrix}_{3\times1} + \begin{pmatrix} b_1 \\ b_2 \\ b_3 \\ b_4 \\ b_5 \\ b_6 \\ b_7 \\ b_8 \end{pmatrix}_{8\times1} \tag{8}$$

The node enters the weighted sum into the activation function (the sigmoid function) and generates its output as in Eq. (9):

$$\begin{pmatrix} o_1 \\ o_2 \\ o_3 \\ o_4 \\ o_5 \\ o_6 \\ o_7 \\ o_8 \end{pmatrix}_{8\times1} = \begin{pmatrix} \varphi(v_1) \\ \varphi(v_2) \\ \varphi(v_3) \\ \varphi(v_4) \\ \varphi(v_5) \\ \varphi(v_6) \\ \varphi(v_7) \\ \varphi(v_8) \end{pmatrix}_{8\times1} \tag{9}$$

Eq. (9) is the input of the second layer. We obtain the weighted sum in the second layer, as shown in Eqs. (10) to (11).

$$\mu_i = \sum\sum w_{ij}{}^{(2)} o_j + b_i{}^{(2)} = \sum\sum w_{ij}{}^{(2)} \varphi\left(v_j\right) + b_i{}^{(2)} \tag{11}$$

$$\begin{pmatrix} \mu_1 \\ \mu_2 \end{pmatrix}_{2\times1} = \begin{pmatrix} w_{11}{}^{(2)} & w_{12}{}^{(2)} & w_{13}{}^{(2)} & w_{14}{}^{(2)} & w_{15}{}^{(2)} & w_{16}{}^{(2)} & w_{17}{}^{(2)} & w_{18}{}^{(2)} \\ w_{21}{}^{(2)} & w_{22}{}^{(2)} & w_{23}{}^{(2)} & w_{24}{}^{(2)} & w_{25}{}^{(2)} & w_{26}{}^{(2)} & w_{27}{}^{(2)} & w_{28}{}^{(2)} \end{pmatrix}_{2\times8} \begin{pmatrix} \varphi(v_1) \\ \varphi(v_2) \\ \varphi(v_3) \\ \varphi(v_4) \\ \varphi(v_5) \\ \varphi(v_6) \\ \varphi(v_7) \\ \varphi(v_8) \end{pmatrix}_{8\times1} + \begin{pmatrix} b_1{}^{(2)} \\ b_2{}^{(2)} \end{pmatrix}_{2\times1} \tag{12}$$

The neuron enters the weight matrix into the linear function and generates its output. The output activation function determines neuron behavior and can be written as in Eq. (13):

$$y = \begin{pmatrix} \psi(\mu_1) \\ \psi(\mu_2) \end{pmatrix}_{2x1} = \psi \left(\begin{pmatrix} w_{11}{}^{(2)} & w_{12}{}^{(2)} & w_{13}{}^{(2)} & w_{14}{}^{(2)} & w_{15}{}^{(2)} & w_{16}{}^{(2)} & w_{17}{}^{(2)} & w_{18}{}^{(2)} \\ w_{21}{}^{(2)} & w_{22}{}^{(2)} & w_{23}{}^{(2)} & w_{24}{}^{(2)} & w_{25}{}^{(2)} & w_{26}{}^{(2)} & w_{27}{}^{(2)} & w_{28}{}^{(2)} \end{pmatrix}_{2\times 8} \begin{pmatrix} \varphi(v_1) \\ \varphi(v_2) \\ \varphi(v_3) \\ \varphi(v_4) \\ \varphi(v_5) \\ \varphi(v_6) \\ \varphi(v_7) \\ \varphi(v_8) \end{pmatrix}_{8\times 1} + \begin{pmatrix} b_1{}^{(2)} \\ b_2{}^{(2)} \end{pmatrix}_{2\times 1} \right) \tag{13}$$

The aim of training the network in this method was to adjust the weights. The weights were adjusted by minimizing the sum of the squares. The neural network was trained by providing input and output designs to it. We used the back-propagation learning algorithm and neural network models to make the model. This algorithm updates the weight values when the performance function rapidly decreases.

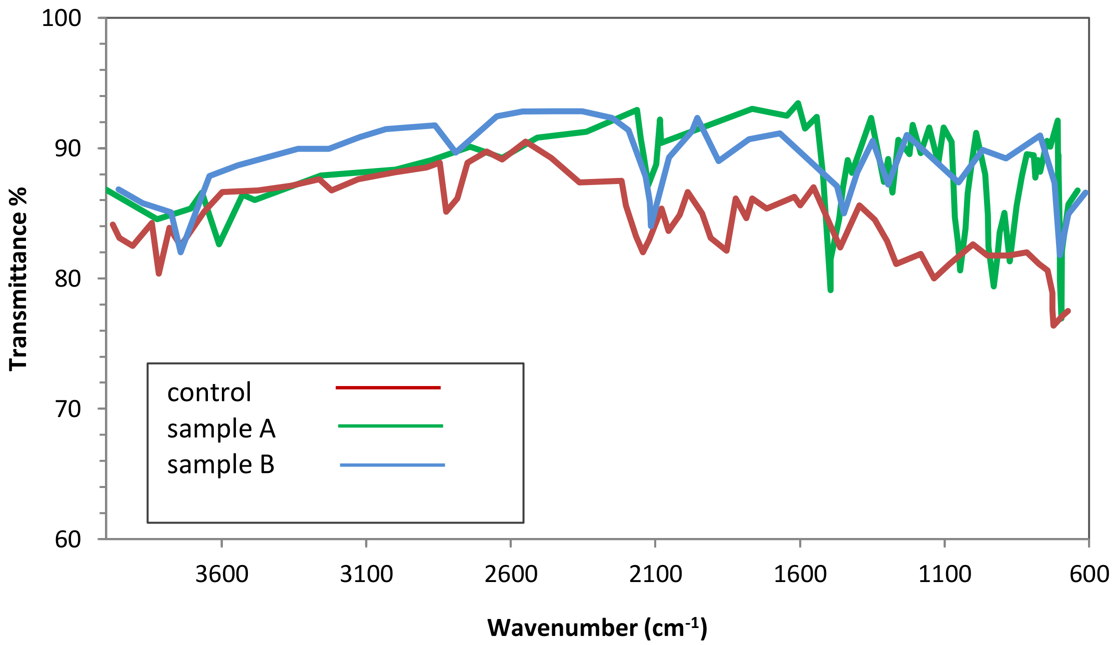

Figure 3. FT-IR spectra of control and plasma-treated T.C. fabric.

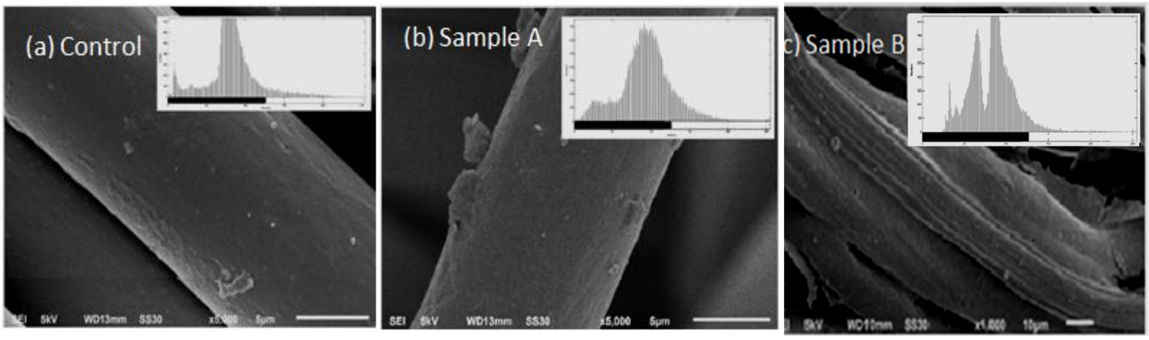

Figure 4. SEM photomicrographs of polyester-cotton fabrics: (a) control (without plasma treatment), (b) treated fabric by plasma for sample A (4.5 cm, 2 minutes, and 3 kV), and (c) treated fabric by plasma for sample B (4.5 cm, 3 minutes, and 3 kV).

RESULTS AND DISCUSSION

In this study, we used FT-IR spectral imaging in conjunction with neural network-based image segmentation to quickly and accurately identify surface roughness and percent transmission with FT-IR of the implication of plasma radiation on textile polymers. Data analysis entails pre-processing quality testing and machine learning algorithms for segmenting FT-IR spectral images and surface roughness with SEM. Data obtained during the experimentation and testing process using ANN are given in Table 1. Table 1 shows data obtained during the experimentation and testing process for control fabric without plasma treatment with red color, treated fabric by plasma for sample A at 4.5 cm, 2 minutes, and 3 kV with green color, and (c) treated fabric by plasma for sample B at 4.5 cm, 3 minutes, and 3 kV with blue color.

Table 1. Data obtained during the experimentation and testing process: (red) control, (green) treated fabric by plasma for sample A (4.5 cm, 2 minutes, and 3 kV), and (blue) treated fabric by plasma for sample B (4.5 cm, 3 minutes, and 3 kV).

No.	Voltage (kV)	Time (minutes)	Wavenumber (cm^{-1})	Actual T%	Actual S.R	ANN T% 4 nodes	ANN S.R	ANN T% 8 Nodes	ANN S.R
1	3	2	4000	86	0.5	84.90633	0.428649	85.58433	0.813143
2	3	2	3823	84	0.5	84.85023	0.441256	85.09615	0.798877
3	3	2	3707	85	0.5	84.89492	0.447586	85.07156	0.78819
4	3	2	3669	86	0.5	84.92369	0.449375	85.13253	0.784389
5	3	2	3609	80	0.5	84.98372	0.451896	85.29849	0.778151
6	3	2	3528	86	0.5	85.09356	0.454675	85.64293	0.769435
7	3	2	3485	84	0.5	85.16549	0.455848	85.87107	0.764765
8	3	2	3256	87	0.5	85.70586	0.458787	87.32776	0.741384
9	3	2	2999	88	0.5	86.58662	0.45918	88.81477	0.721713
10	3	2	2873	89	0.5	87.08436	0.460279	89.36008	0.714985
11	3	2	2740	90	0.5	87.62082	0.462485	89.80335	0.709683
12	3	2	2630	89	0.5	88.05261	0.464956	90.08098	0.706469
13	3	2	2508	90	0.5	88.50114	0.46814	90.31113	0.703913
14	3	2	2339	91	0.5	89.0437	0.472955	90.52151	0.701656

15	3	2	2163	92	0.5	89.47242	0.478141	90.62691	0.699606
16	3	2	2150	90	0.5	89.49692	0.478524	90.62992	0.699378
17	3	2	2141	89	0.5	89.5132	0.47879	90.63156	0.699207
18	3	2	2123	87	0.5	89.54406	0.47932	90.63373	0.698825
19	3	2	2097	88	0.5	89.58443	0.480085	90.63407	0.698162
20	3	2	2084	92	0.5	89.60265	0.480467	90.63291	0.697771
21	3	2	2080	90	0.5	89.60799	0.480585	90.63237	0.697642
22	3	2	1765	93	0.5	89.5121	0.489605	90.10398	0.651618
23	3	2	1646	92	0.5	89.14073	0.492851	89.53917	0.604743
24	3	2	1605	93	0.5	88.96465	0.493943	89.31774	0.58761
25	3	2	1582	91	0.5	88.85524	0.494549	89.19371	0.578553
26	3	2	1541	92	0.5	88.64182	0.495618	88.97881	0.564123
27	3	2	1519	87	0.5	88.51794	0.496185	88.86863	0.557525
28	3	2	1509	84	0.5	88.45956	0.496441	88.81998	0.554822
29	3	2	1494	79	0.5	88.36962	0.496823	88.74879	0.55113
30	3	2	1494	81	0.5	88.36962	0.496823	88.74879	0.55113
31	3	2	1464	84	0.5	88.18161	0.497582	88.61295	0.545074
32	3	2	1452	86	0.5	88.1035	0.497883	88.56102	0.543146
33	3	2	1434	89	0.5	87.98343	0.498331	88.48558	0.540774
34	3	2	1419	88	0.5	87.88082	0.498702	88.42483	0.539257
35	3	2	1354	92	0.5	87.41274	0.500282	88.17945	0.537038
36	3	2	1310	87	0.5	87.0784	0.501324	88.02414	0.538871
37	3	2	1294	89	0.5	86.95419	0.501698	87.96866	0.540061
38	3	2	1280	86	0.5	86.8446	0.502022	87.92027	0.541292
39	3	2	1260	90	0.5	86.68682	0.502481	87.85112	0.543322
40	3	2	1221	89	0.5	86.37623	0.503361	87.71488	0.548003
41	3	2	1209	91	0.5	86.2802	0.503628	87.67229	0.54959
42	3	2	1182	89	0.5	86.06394	0.504222	87.57481	0.553324
43	3	2	1153	91	0.5	85.83208	0.504849	87.46696	0.557481
44	3	2	1120	88	0.5	85.56988	0.505549	87.33943	0.562221
45	3	2	1102	91	0.5	85.42802	0.505924	87.26741	0.564744
46	3	2	1075	90	0.5	85.21726	0.506478	87.15578	0.568361
47	3	2	1069	87	0.5	85.1708	0.5066	87.13036	0.569129
48	3	2	1064	84	0.5	85.1322	0.506701	87.10899	0.569757
49	3	2	1053	82	0.5	85.04766	0.506922	87.06141	0.571098
50	3	2	1045	80	0.5	84.98652	0.507081	87.02628	0.572034

51	3	2	1028	83	0.5	84.8576	0.507417	86.95017	0.573904
52	3	2	1019	86	0.5	84.78993	0.507593	86.90904	0.574822
53	3	2	1003	89	0.5	84.67069	0.507903	86.83446	0.576315
54	3	2	990	91	0.5	84.57483	0.508152	86.77244	0.577388
55	3	2	958	88	0.5	84.343	0.508753	86.61413	0.579424
56	3	2	950	84	0.5	84.286	0.508901	86.57326	0.579787
57	3	2	948	82	0.5	84.27181	0.508938	86.56296	0.579867
58	3	2	929	79	0.5	84.13821	0.509284	86.46344	0.580432
59	3	2	916	81	0.5	84.0481	0.509518	86.39357	0.580597
60	3	2	908	83	0.5	83.99317	0.50966	86.34984	0.580604
61	3	2	892	85	0.5	83.88453	0.509942	86.26068	0.580396
62	3	2	873	81	0.5	83.75761	0.510271	86.15178	0.579744
63	3	2	850	85	0.5	83.60703	0.510661	86.01548	0.578335
64	3	2	831	87	0.5	83.48513	0.510977	85.89907	0.576632
65	3	2	814	89	0.5	83.37795	0.511254	85.79192	0.574678
66	3	2	791	89	0.5	83.23572	0.511621	85.64235	0.571361
67	3	2	785	87	0.5	83.19913	0.511715	85.60245	0.570366
68	3	2	775	89	0.5	83.13861	0.511871	85.53512	0.568584
69	3	2	769	88	0.5	83.10258	0.511963	85.49422	0.56744
70	3	2	746	90	0.5	82.96632	0.512312	85.33392	0.562534
71	3	2	733	90	0.5	82.89058	0.512505	85.24082	0.559387
72	3	2	708	92	0.5	82.7474	0.512867	85.05663	0.552563
73	3	2	707	86	0.5	82.74174	0.512881	85.04911	0.552269
74	3	2	705	89	0.5	82.73043	0.51291	85.03406	0.551675
75	3	2	701	83	0.5	82.70787	0.512966	85.00382	0.550468
76	3	2	701	79	0.5	82.70787	0.512966	85.00382	0.550468
77	3	2	695	76	0.5	82.67418	0.513051	84.95813	0.548608
78	3	2	692	83	0.5	82.65739	0.513093	84.93513	0.547655
79	3	2	692	82	0.5	82.65739	0.513093	84.93513	0.547655
80	3	2	671	85	0.5	82.54109	0.513382	84.77134	0.540565
81	3	2	639	86	0.5	82.36756	0.513807	84.51218	0.528335
82	0	0	3976	84	0	83.13924	0.023674	82.87048	0.01363
83	0	0	3953	83	0	83.21249	0.023381	82.88456	0.005738
84	0	0	3907	82	0	83.36981	0.022681	82.93991	-0.00905
85	0	0	3841	84	0	83.61922	0.021397	83.08179	-0.02818
86	0	0	3818	80	0	83.71219	0.020869	83.14823	-0.03434

87	0	0	3780	83	0	83.87198	0.019908	83.27686	-0.044
88	0	0	3741	82	0	84.04317	0.018811	83.43277	-0.0533
89	0	0	3660	85	0	84.41717	0.016228	83.83028	-0.07092
90	0	0	3598	86	0	84.71425	0.014064	84.19634	-0.08308
91	0	0	3475	86	0	85.30414	0.009744	85.04916	-0.10434
92	0	0	3359	87	0	85.81734	0.00624	85.93727	-0.12112
93	0	0	3262	87	0	86.17566	0.004038	86.65763	-0.13235
94	0	0	3220	86	0	86.30293	0.003304	86.94018	-0.13624
95	0	0	3127	87	0	86.5126	0.002104	87.45322	-0.14228
96	0	0	3000	88	0	86.62227	0.001225	87.79323	-0.14337
97	0	0	2892	88	0	86.5589	0.000945	87.68783	-0.13625
98	0	0	2892	88	0	86.5589	0.000945	87.68783	-0.13625
99	0	0	2845	88	0	86.493	0.000909	87.53497	-0.13057
100	0	0	2822	85	0	86.45374	0.000906	87.44032	-0.1272
101	0	0	2784	86	0	86.38033	0.000916	87.26025	-0.12078
102	0	0	2749	88	0	86.30484	0.000939	87.07366	-0.11394
103	0	0	2683	89	0	86.14797	0.001009	86.68924	-0.09868
104	0	0	2629	89	0	86.01182	0.00108	86.3655	-0.08405
105	0	0	2548	90	0	85.80672	0.001194	85.90517	-0.05894
106	0	0	2460	89	0	85.59696	0.001306	85.47854	-0.02831
107	0	0	2363	87	0	85.3939	0.00139	85.11791	0.007734
108	0	0	2216	87	0	85.14867	0.001397	84.76849	0.061921
109	0	0	2201	85	0	85.12734	0.001388	84.74348	0.067166
110	0	0	2166	83	0	85.07963	0.001358	84.69114	0.079075
111	0	0	2143	82	0	85.04965	0.001331	84.66086	0.086624
112	0	0	2120	83	0	85.02057	0.001299	84.63346	0.093931
113	0	0	2077	85	0	84.96802	0.001225	84.58884	0.106882
114	0	0	2054	83	0	84.94055	0.001177	84.56794	0.113405
115	0	0	2016	84	0	84.89557	0.001084	84.53694	0.123523
116	0	0	1989	86	0	84.86353	0.001008	84.51699	0.130192
117	0	0	1938	85	0	84.80168	0.00084	84.48215	0.141552
118	0	0	1908	83	0	84.76384	0.000725	84.46235	0.147444
119	0	0	1854	82	0	84.69159	0.000489	84.42536	0.156483
120	0	0	1823	86	0	84.64698	0.000335	84.40191	0.160701
121	0	0	1784	84	0	84.58688	0.000123	84.36827	0.164908
122	0	0	1765	86	0	84.55577	1.12E-05	84.3496	0.166477

123	0	0	1715	85	0	84.46738	-0.00031	84.29065	0.168925
124	0	0	1645	86	0	84.32534	-0.00082	84.17423	0.167499
125	0	0	1618	86	0	84.26406	-0.00104	84.115	0.165134
126	0	0	1599	85	0	84.21858	-0.0012	84.06747	0.162777
127	0	0	1552	87	0	84.09709	-0.00162	83.92628	0.154248
128	0	0	1460	82	0	83.81838	-0.00256	83.53913	0.125623
129	0	0	1394	85	0	83.58096	-0.00333	83.17469	0.096604
130	0	0	1340	84	0	83.36077	-0.00402	82.84146	0.070354
131	0	0	1298	82	0	83.1721	-0.00459	82.57429	0.050286
132	0	0	1267	81	0	83.02254	-0.00503	82.37806	0.036449
133	0	0	1182	81	0	82.56457	-0.00634	81.85858	0.005275
134	0	0	1136	80	0	82.2857	-0.00711	81.5873	-0.00705
135	0	0	1082	81	0	81.9288	-0.00807	81.26784	-0.01794
136	0	0	1001	82	0	81.3307	-0.00962	80.7582	-0.02889
137	0	0	950	81	0	80.91394	-0.01066	80.40044	-0.03362
138	0	0	877	81	0	80.26187	-0.01224	79.81468	-0.03878
139	0	0	815	82	0	79.65634	-0.01366	79.23215	-0.04243
140	0	0	773	81	0	79.21943	-0.01467	78.78625	-0.04476
141	0	0	742	80	0	78.88339	-0.01544	78.42845	-0.04648
142	0	0	727	78	0	78.71676	-0.01582	78.24625	-0.04733
143	0	0	727	77	0	78.71676	-0.01582	78.24625	-0.04733
144	0	0	723	76	0	78.67188	-0.01592	78.19665	-0.04755
145	0	0	692	77	0	78.31794	-0.01671	77.7976	-0.04933
146	0	0	672	77	0	78.08393	-0.01724	77.52626	-0.05051
147	3	3	3957	86	1	84.69307	0.957857	83.59436	0.778973
148	3	3	3873	85	1	84.90503	0.96072	84.5388	0.768155
149	3	3	3776	85	1	85.19612	0.963141	85.5792	0.756509
150	3	3	3741	86	1	85.31453	0.963783	85.93393	0.752602
151	3	3	3642	87	1	85.69114	0.965021	86.86261	0.74256
152	3	3	3543	88	1	86.13312	0.965673	87.66891	0.734151
153	3	3	3335	89	1	87.2798	0.9671	88.95849	0.722146
154	3	3	3229	89	1	87.96465	0.968611	89.42623	0.719031
155	3	3	3121	90	1	88.70655	0.970799	89.7941	0.718027
156	3	3	3032	91	1	89.32692	0.972991	90.02767	0.718981
157	3	3	2862	91	1	90.43121	0.977741	90.33281	0.726089
158	3	3	2791	89	1	90.81837	0.979822	90.41486	0.731549

159	3	3	2649	92	1	91.37229	0.983974	90.51241	0.748082
160	3	3	2560	92	1	91.52986	0.98651	90.53299	0.762984
161	3	3	2452	92	1	91.49771	0.989472	90.51933	0.786458
162	3	3	2353	92	1	91.25479	0.992051	90.47106	0.813291
163	3	3	2250	92	1	90.81437	0.994579	90.38471	0.845807
164	3	3	2192	91	1	90.50178	0.995928	90.31894	0.865386
165	3	3	2134	87	1	90.15788	0.99722	90.23912	0.885049
166	3	3	2119	85	1	90.06546	0.997545	90.21588	0.890037
167	3	3	2116	84	1	90.04685	0.997609	90.21109	0.891027
168	3	3	2053	89	1	89.65025	0.998927	90.09839	0.910789
169	3	3	1974	91	1	89.15469	1.00048	89.91576	0.930882
170	3	3	1954	92	1	89.03271	1.000855	89.86015	0.934712
171	3	3	1880	89	1	88.60339	1.002178	89.61293	0.942846
172	3	3	1775	90	1	88.07514	1.003877	89.1381	0.935148
173	3	3	1668	91	1	87.65329	1.005384	88.55979	0.908898
174	3	3	1472	87	1	87.16559	1.007531	87.72436	0.866913
175	3	3	1448	84	1	87.12588	1.007737	87.65712	0.864281
176	3	3	1402	88	1	87.05843	1.008095	87.54513	0.860403
177	3	3	1347	90	1	86.9897	1.008462	87.43371	0.857142
178	3	3	1294	87	1	86.93193	1.008748	87.34162	0.854682
179	3	3	1230	91	1	86.86793	1.009006	87.24082	0.851748
180	3	3	1050	87	1	86.67441	1.00919	86.95064	0.838256
181	3	3	968	89	1	86.55854	1.008998	86.78934	0.827713
182	3	3	887	89	1	86.4164	1.008631	86.59876	0.813719
183	3	3	768	90	1	86.14641	1.007759	86.2438	0.78544
184	3	3	719	87	1	86.01148	1.007281	86.06591	0.770707
185	3	3	700	81	1	85.95519	1.007077	85.99124	0.764457
186	3	3	670	84	1	85.86169	1.006733	85.86648	0.753946

Modeling with four neurons in a hidden layer

Three parameters were used as independent variables (x_i) in this model. Where x_1, x_2, and x_3 represented voltage, exposure time, and wavenumber, respectively. Fabric surface roughness (S.R.) and percent transmission (T percent) were predicted as output parameters. The neural network performs four nodes (neurons) in the hidden layer to receive three parameters (x_1, x_2, x_3). This study uses 20 iterations and 186 samples for three parameters, as shown in Table 1, and the model's results are shown in Figures 5 and 6. In this research, we used the R-squared (R^2) coefficient to show the satisfactory adjustment of the proposed model to the experimental data. According to this study, the model is appropriate for determining fabric surface roughness (S.R.) and percent transmission (T%). Based on this research, the values of R^2 for determining fabric surface roughness (S.R.) and percent transmission (T%) were 99.79 percent and 67.18 percent. Figure 5 is a graph of the actual and predicted values obtained using an artificial neural network (ANN) to calculate fabric surface roughness (S.R.) and percent transmittance (T%) from Table 1 using a number of 186 data to determine. Figure 6 shows the neural network's performance and R-squared values for each sample. This figure depicts that the ANN results closely match the experiments, which have a value of 67.18 percent for the prediction of percent transmission and 99.79 percent for the prediction of fabric surface roughness (S.R.). Figure 6 depicts the model's validation using R-squared, which measures how the model represents the observed result as the ratio of variation to total output described by the model.

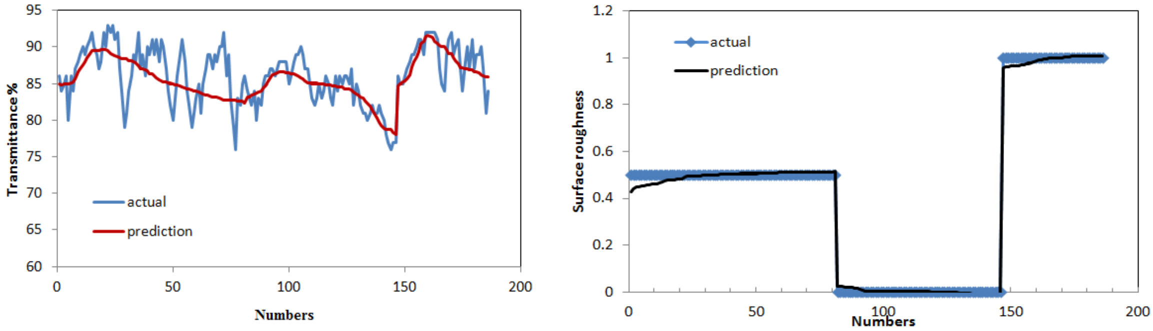

Figure 5. the result of the model with four neurons in a hidden layer.

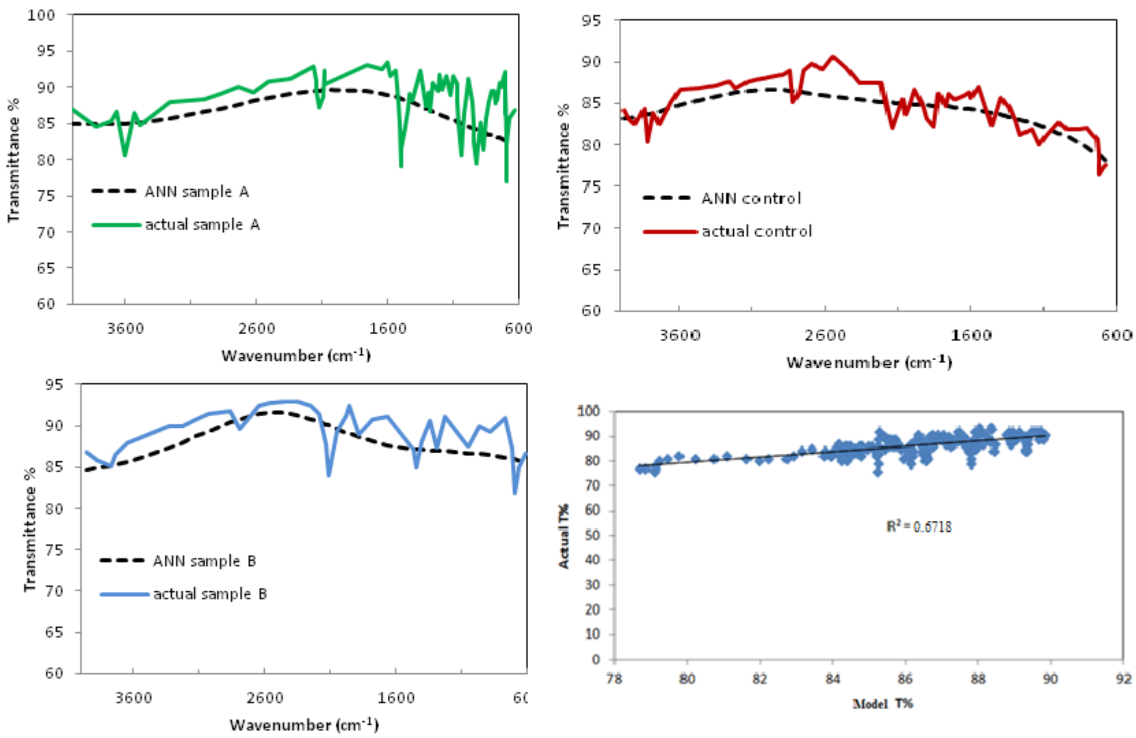

Figure 6. The result of the model with four neurons in a hidden layer for control, sample A, and sample B, with an R-squared value of 67.18% of percent transmission (T%).

Using Eq. (2) and Eq. (6), the artificial neural network can be written in Eqs. (14) and (15) as follows:

$$\begin{pmatrix} v_1 \\ v_2 \\ v_3 \\ v_4 \end{pmatrix}_{4\times1} = \begin{pmatrix} 6.1867 & 0.0402 & -8.0696 \\ 0.0815 & 0.2555 & 0.8037 \\ -0.3246 & -2.5767 & 6.5510 \\ 3.5672 & 1.0812 & -2.1649 \end{pmatrix}_{4\times3} \begin{pmatrix} x_1 \\ x_2 \\ x_3 \end{pmatrix}_{3\times1} + \begin{pmatrix} 6.2371 \\ 1.5614 \\ -2.0057 \\ 5.9958 \end{pmatrix}_{4\times1} \tag{14}$$

$$y = \begin{pmatrix} \psi(\mu_1) \\ \psi(\mu_2) \end{pmatrix}_{2x1} = \psi\left(\begin{pmatrix} -0.4186 & 2.3299 & -0.3393 & 0.5174 \\ 0.5426 & 2.8232 & -0.2597 & -0.2171 \end{pmatrix}_{2\times4} \begin{pmatrix} \varphi(v_1) \\ \varphi(v_2) \\ \varphi(v_3) \\ \varphi(v_4) \end{pmatrix}_{4\times1} + \begin{pmatrix} -2.078 \\ -2.828 \end{pmatrix}_{2\times1} \right) \tag{15}$$

Where the terms $\varphi(v)$ and $\psi(\mu)$ are the sigmoid function and linear function, v_i is the weighted sum of the first layer, μ_i is the weighted sum of the second layer, w_{ij} and ${w_{ij}}^2$ are the weight matrices of the first and second layers, respectively.

Modeling with eight neurons in a hidden layer

Three variables were used as independent variables (x_i) in this model. Where x_1, x_2, and x_3 represented voltage, exposure time, and wavenumber, respectively. Fabric surface roughness (S.R.) and percent transmission (T%) were predicted as output parameters. The neural network performs four nodes (neurons) in the hidden layer to receive three variables (x_1, x_2, x_3). This study uses 20 iterations and 186 samples for three variables, as shown in Table 1, and the model's results are shown in Figures 7 and 8. In this research, we used the R-squared (R^2) coefficient to show the satisfactory adjustment of the proposed model to the experimental data. According to this study, the model is appropriate for determining fabric surface roughness (S.R.) and percent transmission (T%). Based on this research, the values of R^2 for determining fabric surface roughness (S.R.) and percent transmission (T%) were 85.68 percent and 51.57 percent, respectively. Figure 7 depicts a plot of the actual and predicted values obtained by using an artificial neural network (ANN) to determine the fabric surface roughness (S.R.) and percent transmission (T%) from Table 1 using a number of 186 data to determine. Figure 8 shows the neural network's performance and R-squared values for each sample. This figure depicts that the ANN results closely match the experiments, which have a value of 51.57 percent for the prediction of percent transmission and 85.68 percent for the prediction of fabric surface roughness (S.R.). Figure 8 depicts the model's validation using R-squared, which measures how the model represents the observed result as the ratio of variation to total output described by the model.

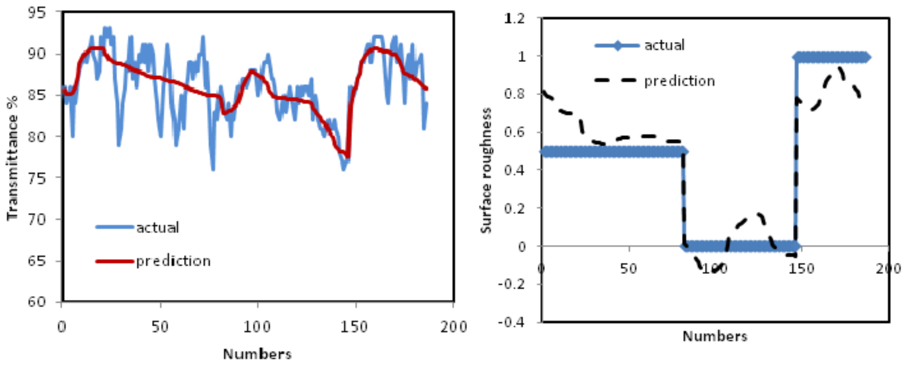

Figure 7. the result of the model with eight neurons in a hidden layer

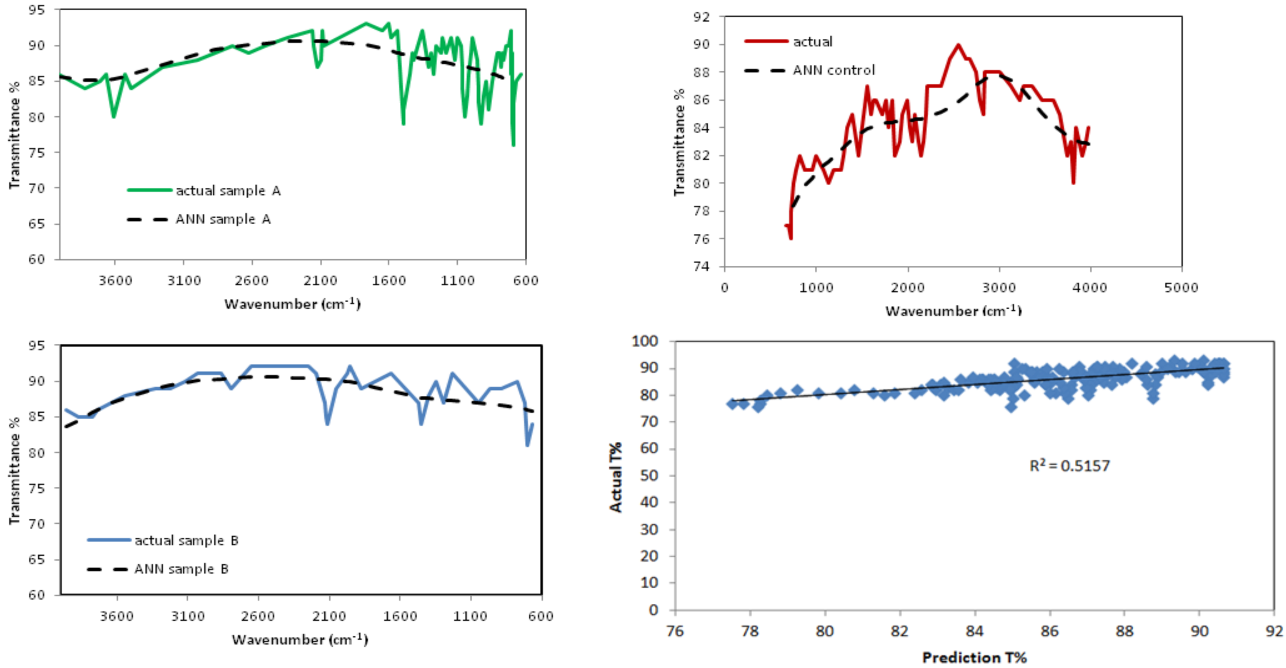

Figure 8. The result of the model with four neurons in a hidden layer for control, sample A, and sample B with an R-squared value of 51.57% of percent transmission (T%).

Using Eq. (8) and Eq. (13), the artificial neural network can be written in Eqs. (16) and (17) as follows:

$$\begin{pmatrix} v_1 \\ v_2 \\ v_3 \\ v_4 \\ v_5 \\ v_6 \\ v_7 \\ v_8 \end{pmatrix}_{8\times1} = \begin{pmatrix} -2.4570 & 0.5778 & -0.7934 \\ -3.0159 & -2.2867 & 0.9089 \\ -0.3063 & -0.3996 & 7.0312 \\ 3.0274 & 0.5378 & 2.4718 \\ 2.4789 & 2.9556 & -2.9792 \\ 2.9879 & -2.7177 & 2.9888 \\ -0.7545 & 3.0964 & -3.9137 \\ 0.1591 & -0.8067 & 2.3684 \end{pmatrix}_{8\times3} \begin{pmatrix} x_1 \\ x_2 \\ x_3 \end{pmatrix}_{3\times1} + \begin{pmatrix} -7.0572 \\ 0.9201 \\ 3.3044 \\ -0.0568 \\ 1.8688 \\ 0.1952 \\ 3.3884 \\ -1.8118 \end{pmatrix}_{8\times1} \tag{16}$$

$$y = \begin{pmatrix} \psi(\mu_1) \\ \psi(\mu_2) \end{pmatrix}_{2x1} = \psi\left(\begin{pmatrix} -0.4935 & -0.7230 & 0.1260 & 0.9263 & -1.3573 & 0.0811 & -0.7155 & -1.072 \\ 0.0482 & 0.3584 & 0.2499 & 1.3824 & -0.0945 & -0.4546 & 0.0522 & 0.2013 \end{pmatrix} + \begin{pmatrix} -0.5846 \\ -0.1379 \end{pmatrix}_{2\times 1} \right) \quad (17)$$

Based on this research, the model that used four nodes (neurons) in the hidden layer, three input parameters (x_1, x_2, x_3), a constant learning rate (α=0.9), and 20 iterations is appropriate for determining fabric surface roughness (S.R.) and percent transmission (T%). Based on this research, the values of R^2 of the ANN model that used four nodes in the hidden layer for determining fabric surface roughness (S.R.) and percent transmission (T%) were 99.79 percent and 67.18 percent, respectively. The new major finding of the study is that we used the ANN to model the FT-IR spectral information and fabric surface roughness of the plasma treatment on polyester-cotton fabrics simultaneously using Eq. (15). According to the findings, plasma voltage, plasma exposure time, and electrode distance, all affect the nano surface structure and chemical structure of the fabric. Although the chemical bond analysis cannot be determined in detail on FT-IR results, the FT-IR spectral model with ANN can be used to classify fabrics with and without plasma treatment. As shown in Figure 6, the ANN simulation results show different patterns in the FTIR spectra for the control tissue, Sample A and Sample B. The FT-IR spectra of plasma-treated and non-plasma-treated polymers have been described as reproducible fingerprint-like patterns and vary by polymer type. In this study, we have classified or identified the effect of plasma on textile fabric. According to Morent et al., measurements of polymer chemical bonding using Fourier transform infrared spectroscopy (FT-IR) play an essential and unavoidable role in applying surface modification and work of adhesion with plasma technology in several nanotechnology studies [5]. The results showed that the developed ANNs could accurately predict the experimental data in detail. This study is significant because it uses artificial intelligence to calculate and simulate the chemical bonding information from FT-IR measurements and fabric surface roughness of plasma treatment on textile fabrics.

CONCLUSIONS

FT-IR spectra from plasma-treated and untreated fabrics could give sufficient information to identify fabric surface roughness using Artificial Neural Networks. ANN was an excellent tool for determining the surface roughness of a fabric. ANN allowed us to identify the wave number and structure of chemical compounds with the most significant influence on surface roughness identification. According to this study, the model that used four nodes (neurons) in the hidden layer, three input parameters (x_1,x_2,x_3), and 20 iterations was appropriate for determining fabric surface roughness (S.R.) and percent transmission (T%). Based on this research, the values of R^2 for determining fabric surface roughness (S.R.) and percent transmission (T%) were 99.79 percent and 67.18 percent, respectively. The new major finding of the study is that for the first time, we used ANN to accurately model the plasma treatment on polyester-cotton fabrics and the FT-IR spectral measurements. This research is essential because we used artificial intelligence to calculate and simulate chemical bonding data from FT-IR measurements and fabric surface roughness of plasma treatment on textile fabrics. The scientific implementation of this research will encourage practitioners, researchers, and engineers to understand the effects of plasma on the chemical structure of textile materials.

ACKNOWLEDGMENTS

The authors expressed their deepest gratitude to the Republic of Indonesia's Ministry of Industry for providing sufficient facilities. We also thank our colleagues who assisted us during the research and analysis.

REFERENCES

[1] D. L. Francisco, L. B. Paiva, and W. Aldeia, "Advances in Polyamide Nanocomposites: A Review.," *Polymer Composites.*, vol. 40, no. 3, pp. 851- 870, 2018.

[2] V. Putra, J. Mohamad, D. Arief and Y. Yusuf, "Surface modification of polyester-cotton (T.C. 70%) fabric by corona discharged plasma with tip cylinder electrode configuration-assisted coating carbon black conductive ink for electromagnetic shielding fabric," *Arab Journal of Basic and Applied Sciences,* vol. 28, no. 1, p. 272–282, vol. 28, no. 1, pp. 272–282, 2021.

[3] M. Molakarimi, M. Khajeh Mehrizi and A. Haji, "Effect of plasma treatment and grafting of B-cyclodextrin on color properties of wool fabric dyed with shrimp shell extract," *The Journal of the Textile Institute,* vol. 107, no. 10, pp. 1314-1321, 2016.

[4] H. Rausher, M. Perucca and G. & Buyle, Plasma technology for hyperfunctionals surfaces, Weinheim: Wiley-VCH, 2010.

[5] R. Morent, N. De Geyter, J. Verschuren, K. De Clerck, P. Kiekens and C. Leys, "Non-thermal plasma treatment of textiles," *Surface and Coatings Technology,* vol. 202, no. 14, pp. 3427–3449, 2008.

[6] M. R. Alexander, S. Payan and T. M. Duc, "Interfacial interactions of plasma-polymerized acrylic acid and an oxidized aluminium surface investigated using XPS, FTIR and poly(acrylic acid) as a model compound," *Surface and Interface Analysis,* vol. 26, no. 13, pp. 961-973, 1998.

[7] N. Bhat, A. Netravali, A. Gore, M. Sathianarayanan, G. Arolkar and R. Deshmukh, "Surface modification of cotton fabrics using plasma technology," *Textile Research Journal,* vol. 81, no. 10, pp. 1014-1026, 2011.

[8] B. Paosawatyanyong, K. Kamlangkla and S. Hodak, "Hydrophobic and Hydrophilic Surface Nano-Modification of PET Fabric by Plasma Process," *Journal of Nanoscience and Nanotechnology,* vol. 10, no. 11, pp. 7050-7054, 2010.

[9] S. Masaoka, "Plasma sterilization of polyethylene terephthalate bottles by pulsed corona discharge at atmospheric pressure," *Biocontrol Sci,* p. 59, 2007.

[10] F. Leroux, A. Perwuelz, C. Campagne and e. al, "Atmospheric air-plasma treatments of polyester textile structures," *J Adhes Sci Technol,* vol. 20, pp. 939–957, 2006.

[11] C. Murru, C. Chimeno-Trinchet, M. E. Díaz-García, R. Badía-Laíño and A. Fernández-González, "Artificial Neural Network and Attenuated Total Reflectance-Fourier Transform Infrared Spectroscopy to identify the chemical variables related to ripeness and variety classification of grapes for Protected. Designation of Origin wine production," *Computers and Electronics in Agriculture,* vol. 164, pp. 104922, 2019.

[12] W. Q. Z. M. X. J. L. L. K. B. C. M. N. Z. W. Q. M. Nie, M. Xiao, L. Luo, K. Bao, J. K. Chen and B. Li, "FT-IR Spectroscopy and Artificial Neural Network Identification of Fusarium Species," *J. Phytopathology,* vol. 155, no. doi: 10.1111/j.1439-0434.2007.01245.x, pp. 364–367, 2007.

[13] N. Naderi, F. Agend, R. Faridi-Majidi, N. Sharifi-Sanjani and M. Madani, "Prediction of nanofiber diameter and optimization of electrospinning process via response surface methodology," *J. Nanosci. Nanotechnol,* vol. 8, no. 5, pp. 2509–2515, 2008.

[14] T. Padmanabhan, V. Kamaraj, L. Magwood and B. Starly, "Experimental investigation on the operating variables of a near-field electrospinning process via response surface methodology," *J. Manuf. Process,* vol. 13, no. 2, pp. 104–112, 2011.

[15] P. Souza, G. Dotto and N. Salau, "Artificial neural network (ANN) and adaptive neuro-fuzzy interference system (ANFIS) modelling for nickel adsorption onto agro-wastes and commercial activated carbon," *Journal of Environmental Chemical Engineering,* vol. 6, no. 6, pp. 7152-710, 2018.

[16] C. Wang, X. Wang and X. He, " Neural networks model of polypropylene surface modification by air plasma," in *Proceedings of the IEEE International Conference on Automation and Logistic,* Jinan, China, 2007.

[17] A. Majumdar, M. Ciocoiu and M. Blaga, "Modelling of ring yarn unevenness by soft computing approach," *Fibers and Polymers,* vol. 9, no. 2, pp. 210-216, 2008.

[18] O. Demiryurek and E. Koe, "Predicting the tensile strength of polyester/viscose blended open-end rotor spun yarns using artificial neural network and statistical models," *Fibers and Polymers,* vol. 10, no. 2, pp. 237-245, 2009.

[19] M. A. Karimi, P. Pourhakkak, M. Adabi, S. Firoozi, M. Adabi and M. Naghibzadeh, "Using an artificial neural network for the evaluation of the parameters controlling PVA/chitosan electrospun nanofibers diameter," *e-Polymers,* vol. 15(2), no. https://doi.org/10.1515/epoly-2014-0198, pp. 127–38, 2015.

[20] R. Faridi-Majidi, H. Ziyadi, N. Naderi and A. Amani, "Use of artificial neural networks to determine parameters controlling the nanofibers diameter in electrospinning of nylon-6," *J. Appl. Polym. Sci.,* vol. 124, no. 2, pp. 1589–97, 2012.